Sully, J. P. & Campanella, R. G. (1995). *Géotechnique* **45**, No, 2, 267–282

Evaluation of in situ anisotropy from crosshole and downhole shear wave velocity measurements

J. P. SULLY* and R. G. CAMPANELLA†

Downhole and cross hole shear wave velocity determinations are becoming a routine part of dynamic site evaluation studies. The in situ measurements are frequently performed in boreholes using a variety of techniques. A seismic cone system has been developed for determining both downhole and crosshole shear wave velocity. The system consists of a source and two receivers, all embodied in penetrometers. At any depth three different polarized sets of shear wave signals can be generated and are recorded by both receivers, located at different distances from the source. It has been suggested from laboratory tests in large chambers that the measured shear wave velocities can be used to evaluate the in situ stress conditions. Tests have been performed at research sites in Vancouver to evaluate the in situ stress dependence of the measured shear wave velocities. The results of this study suggest that variations in structural anisotropy are the predominant factors controlling the directional shear wave velocities, and almost mask the effect of stress-induced variations.

KEYWORDS: anisotropy; clays; in situ testing; laboratory tests.

Les mesures de vitesse des ondes transversales, le long et entre les trous, font partie intégrante de la routine des études dynamiques d'évaluation des sites. Les mesures in-situ sont très souvent réalisées dans des trous de forages à l'aide de diverses techniques. Le système développé permet de mesurer à la fois, à l'aide d'un cône sismique, les vitesses le long et entre les trous. Ce système est constitué d'une source et de deux récepteurs intégrés à des pénétromètres. Quelle que soit la profondeur, trois différents trains d'ondes polarisées peuvent être générés puis enregistrés par les deux récepteurs situés à une distance variable de la source. Les essais de laboratoire à grande échelle laissent à supposer que les vitesses mesurées permettent d'évaluer les conditions de contrainte in-situ. Des essais ont été réalisés dans des sites d'étude à Vancouver pour évaluer la relation de la vitesse des ondes transversales à la contrainte in-situ. Il ressort de cette étude que cette vitesse est principalement fonction des variations de l'anisotropie structurale qui masquent de ce fait les effets dus aux variations de la contrainte in-situ.

INTRODUCTION

The key parameter in many constitutive models and numerical techniques for evaluating soil response to applied static and dynamic loads is the shear modulus. The shear modulus may be determined from either static or dynamic in situ or laboratory tests. Its magnitude depends on various factors such as stress state, material characteristics and strain level. At small strains (approximately $<10^{-4}\%$), the measured modulus is called the maximum shear modulus (G_0 or G_{max}) and for a given soil can be considered a fundamental soil property. Various studies have shown that G_0 is primarily a function of both stress state and soil fabric (Hardin, 1978; Yu & Richart, 1984, Roesler, 1979; Stokoe, Lee & Knox, 1985)

$$G_0 = f(\sigma', \alpha) \tag{1}$$

where σ' is some measure of the effective stress in the soil and α is a parameter representative of the soil fabric.

According to elastic theory, G_0 can be calculated from the elastic shear wave velocity as given by

$$G_0 = \rho V_s^2 \tag{2}$$

where ρ is the density of the soil and V_s is the elastic shear wave velocity, generated at shear strain amplitudes of $10^{-4}\%$ or less.

Several techniques are currently used to measure V_s both in the laboratory and in the field; these are reviewed by Woods (1978, 1986, 1991). In the field, in situ shear wave velocity measurements are commonly performed using both downhole (DH) and crosshole (XH) procedures. The velocity measurements are usually carried out in one or more boreholes and are relatively expensive to perform. A more recent

Manuscript received 5 October 1992; revised manuscript accepted 4 May 1994.
Discussion on this Paper closes 1 September 1995; for future details see p. ii.
* GEOHIDRA, C.A., Caracas.
† University of British Columbia.

version of the downhole test developed at the University of British Columbia (UBC) uses a cone penetrometer with mounted seismometer, thus eliminating the need for boreholes (Campanella & Robertson, 1984). The seismometer is incorporated into the cone body and used to detect body wave arrivals generated from a seismic source located at the surface. By modifying the equipment set-up, the seismic cone penetration test (SCPT) can also provide XH velocity measurements (Baldi, Bruzzi, Superbo, Battaglio & Jamiolkowski, 1988; Sully & Campanella, 1992). Recently, spectral analysis of surface waves (SASW) has been providing V_s measurements without the need for boreholes or other types of penetration test (Nazarian & Stokoe, 1984; Stokoe & Nazarian, 1985).

The in situ measurement of shear wave velocity by the DH and XH methods using a cone penetrometer is the subject of this Paper. Previous research suggests that so long as sufficient measurements can be made, it may be possible to use the results to index and/or evaluate stress and structural anisotropy in soils. The seismic cone penetration test, usually used for DH measurements, is modified to allow XH measurements to be made at the same time. Details of the modified equipment, test set-up and procedure are presented.

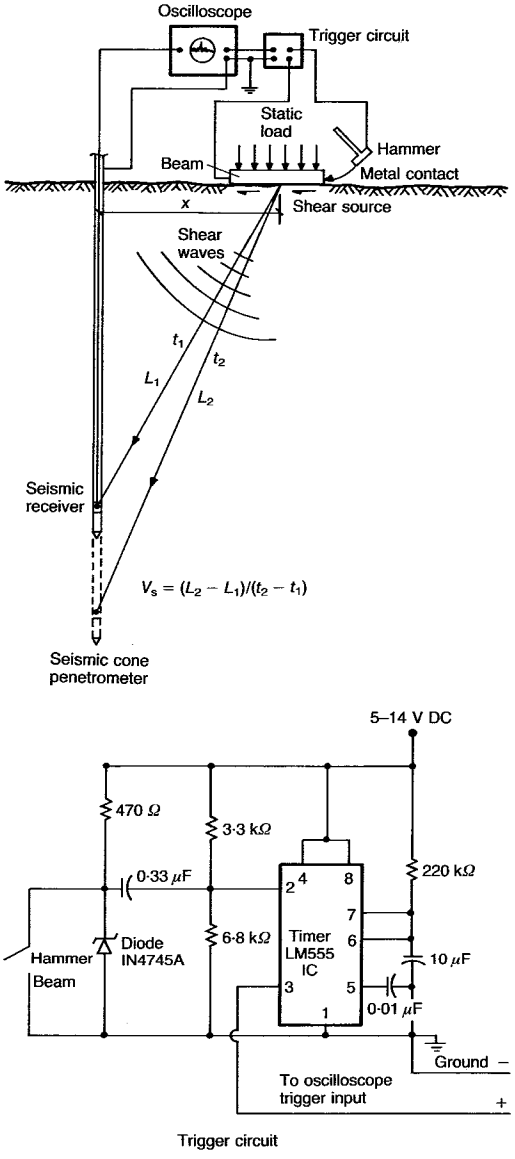

Fig. 1. Arrangement for DH SCPT (Campanella & Stewart, 1991)

SEISMIC CONE PENETRATION TEST

SCPT DH procedure

Campanella & Robertson (1984) developed the DH SCPT to provide a rapid and economic way of performing in situ shear wave velocity measurements. The seismometer is placed horizontally and oriented perpendicular to the source to provide maximum sensitivity to the horizontal component of the surface-generated shear wave. The arrangement for performing the DH SCPT is shown in Fig. 1, which also shows the step trigger circuit. The polarized shear waves are generated at the surface by horizontal striking of a weighted shear beam. For tests performed with the UBC geotechnical testing vehicle, the steel pads on which the truck is supported can be used as a shear beam as the high normal loads provided by the weight of the truck ensure excellent coupling with the ground. Good coupling is essential to ensure that no energy is lost when the shear beam is struck. An advantage of the shear beam method is that the polarized signals can be reversed by striking of the opposite ends of the beam.

The horizontally polarized wave travels essentially vertically from the source to the receiver mounted in the cone. The direction of wave travel (vertical) is perpendicular to the direction of particle motion (horizontal). This type of DH wave is a VH wave.

The SCPT is performed by first pushing the cone to the depth of interest. A horizontal blow to the shear beam is then applied. Hammer contact with the shear beam provides the trigger for the data acquisition system (DAS), which recovers the signal when it arrives at the receiver mounted in the cone. The time for the signal to travel from the ground surface to the cone receiver can then be obtained. Measurement of the

travel times from tests at subsequent depths allows the shear wave velocity profile to be determined from the pseudo-interval time method (Campanella, Robertson & Gillespie, 1986).

The seismic data are recorded on the Nicolet 4094 digital oscilloscope which has a cathode ray tube screen and permits data storage on a floppy disk. The equipment has a 15 bit A/D resolution, a time resolution down to 10 μs and a rise time of less than 1 μs. Detailed information on the equipment currently being used at UBC is given by Campanella & Stewart (1991).

Standard UBC seismic cone

The standard UBC seismic cone consists of a horizontally oriented seismic receiver mounted in the shaft of the 10 cm^2 penetrometer. Several types of receiver have been used during the development of the test, including geophones and accelerometers (piezoceramic and piezoresistive), depending on the objects of the particular study. All three types have been used here.

The geophones are 1·7 cm in diameter and have a natural frequency of 28 Hz. A single geophone is used in the 10 cm^2 cone, whereas a triaxial package is used in the larger 15 cm^2 cone. The piezoceramic bender units are 1·27 cm square, are undamped and have a natural frequency of 3000 Hz. The piezoresistive accelerometers are also undamped and have a 10g range, with a natural frequency of 600 Hz.

Trigger set-up

The trigger set-up is shown in Fig. 1. An electrical circuit is completed when the hammer strikes the metal shear beam. This allows a capacitor to discharge, causing the timer module to generate a pulse of about 2·4 s duration. This duration negates the possible effects of bounces of the hammer. The rise time of the hammer is typically 100 ns. The trigger circuit automatically rearms for the subsequent event.

Shear wave sources

The shear beam is the primary source used for generating the polarized shear waves used in this study. This type of source produces a very clean shear wave with essentially no compression wave. Strain amplitudes in the ground close to the ground surface are generally less than 10^{-2}% and decrease with depth. A 12 kgf hammer with an adjustable swing is in use at present, which produces a highly repeatable and calibrated energy source.

SCPT XH procedure

Using a dual cone system, Baldi *et al.* (1988) modified the DH SCPT in order to perform XH velocity measurements. Two CPT pushing rigs are required; one of the trucks pushes the cone that is used as an energy source while the other rig pushes the receiver cone with a biaxial geophone incorporated (Fig. 2).

The seismic cone test can be performed during routine cone penetration testing. At any particular depth of interest, penetration of both source and receiver cones is halted. A horizontally propagating shear wave with vertical particle motion (HV wave) is generated by striking the top of the rods connected to the source cone. The record of shear wave signal at the receiver cone permits the XH V_s to be calculated. However, as only one receiver cone is used, the shear wave velocity has to be calculated from the first arrival time. The error in this approach may be significant, depending on the quality of the signal and the soil conditions at the test location.

Baldi *et al.* (1988) performed tests with a XH spacing (distance between source and receiver cones) of up to 10 m. Downhole V_s measurements can also be performed at the location of the receiver cone (by generating a VH wave) as described for the standard DH arrangement. Hence both DH and XH velocities can be obtained. The set-up used by Baldi *et al.* (1988) has a disadvantage in that two purpose-designed in situ testing vehicles are required, thus limiting the application of such a procedure to large high-profile projects.

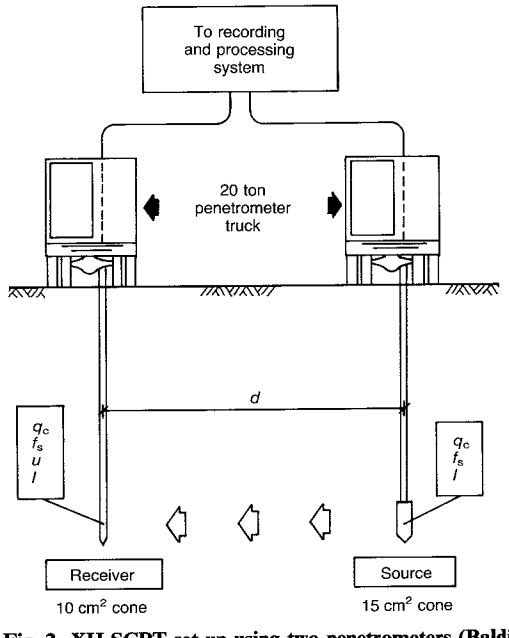

Fig. 2. XH SCPT set-up using two penetrometers (Baldi *et al.*, 1988)

A simple DH and XH set-up has been developed at the University of British Columbia (UBC) which is capable of generating different polarized shear waves so that in situ anisotropy can be examined. The equipment and results obtained at three research sites are described here.

DH-XH SCPT

The DH-XH SCPT set-up developed uses a source and two receivers, all embodied in cone penetrometers. Two receivers are considered necessary to ensure accurate determination of the XH travel times, especially as the XH separation used is small (about 2–4 m). The DH measurement uses a pseudo-interval technique between two different depths and so only one receiver is required for complete interpretation of the data. The source, in the form of a vane cone, was designed so that the horizontally polarized shear wave could be generated with either vertical (HV) or horizontal (HH) particle motion. Details of the 15 cm^2 vane cone used for shear wave generation are shown in Fig. 3; the field test configuration is shown in Fig. 4.

The receiver cones are standard UBC seismic cones which incorporate a single accelerometer package. Trials performed in the laboratory indicated that the single accelerometer package was sufficiently sensitive to the three oriented shear waves to be produced in the field tests, and that for the initial study it would not be necessary to include a triaxial package in the cone. The response of the accelerometer is such that the consequence of recording out-of-plane signals is that the amplitude of the signal is reduced. This reduction depends on the angle between the wave front and the accelerometer orientation. However,

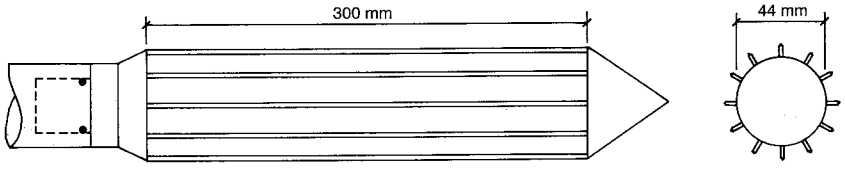

Fig. 3. Vane cone for generating horizontal shear waves in XH test

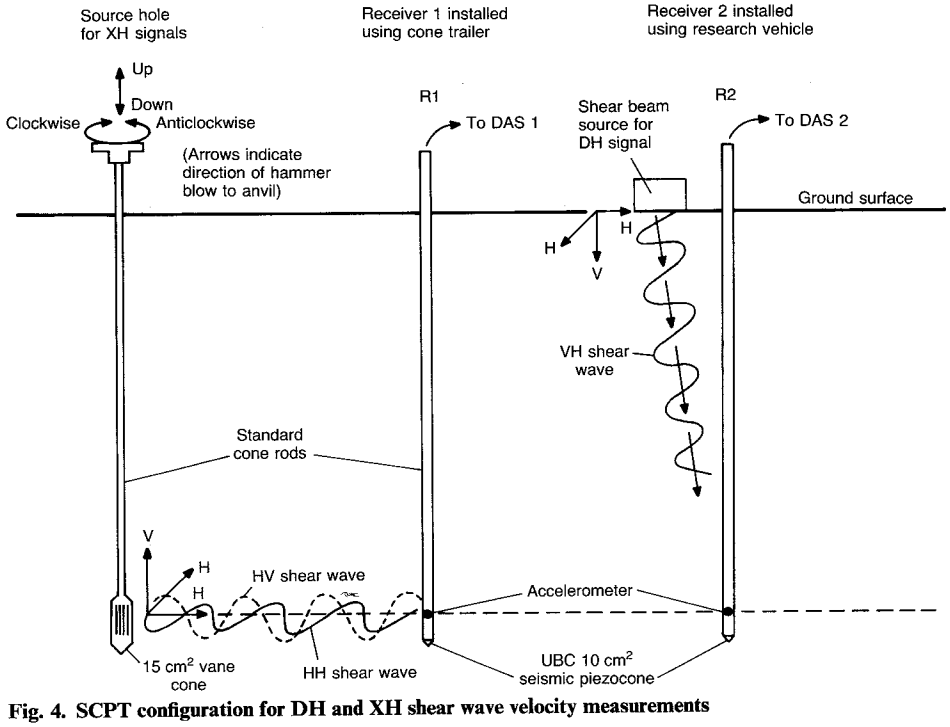

Fig. 4. SCPT configuration for DH and XH shear wave velocity measurements

the evaluated travel times are not sensitive to the alignment effect and the shear wave velocities thus determined are not affected.

The DH-XH SCPT procedure comprises the following steps.

First, a DH SCPT is performed at the required depth interval (usually 0·5 m or 1·0 m) at the location where the source vane cone is to be installed. A standard 10 cm^2 seismic cone is used with no friction reducer.

The 15 cm^2 vane cone used as the source is then installed to a depth of 1 m in this hole (measured to the centre of the vane section). The installation of the 15 cm^2 source cone in a pre-bored smaller diameter hole reduces the force required to penetrate the cone; the slightly larger diameter of the source cone ensures a good contact with the surrounding soil necessary for signal generation.

Two receiver cones (R1 and R2) are then installed along a common line at known distances from the source location, also to a depth of 1 m. Receiver R1 is installed using a 20 ton capacity lightweight trailer equipped with pushing ram. Receiver R2 is installed using the UBC research vehicle (Campanella & Robertson, 1981). (If hard ground conditions are encountered, a slightly undersized cone can be pre-pushed with the UBC truck at the R1 location to facilitate subsequent installation of the receiver cone with the light-weight trailer.) R1 and R2 are connected to separate data acquisition systems (DAS1 and DAS2).

With the three cones at the same depth, the following DH and XH signals are generated

(*a*) DH test at R2 location with oppositely polarized signals (VH) from hits on the left and right sides of the front (or back) pad of the truck

(*b*) XH test with oppositely polarized signals (HV) from vertical up and down hits on rods at the source cone location; the HV wave traces are recorded at both R1 and R2

(*c*) XH test with oppositely polarized signals from clockwise and anticlockwise hits (HH) on cone rods; the HH wave traces are recorded at both R1 and R2 (the blows to the cone rods in (b) and (c) are transmitted to the rods via the anvil screwed into the top of the cone rods (see Fig. 4)

(*d*) all three cones are advanced to the next depth, and steps (a)–(c) are repeated until the final depth of interest is reached.

Multiple hits for each of the signals were used to check repeatability. A horizontal spacing of about 2–3 m between the individual cones was found to give the best results for the sites tested and the particular energy source being used.

INTERPRETATION OF SHEAR WAVE TRACES

Three principal techniques are used for interpreting the shear wave traces obtained from DH and XH SCPT procedures, namely: first shear wave arrival, a crossover or reverse polarity method and a cross-correlation method.

First shear wave arrival

In the first shear wave arrival approach the shear wave velocity is calculated based on the arrival time of the shear wave at the receiver (Stokoe & Woods, 1972). The advantage is that the method can be used when only one receiver is employed in the XH test set-up. The technique is purely visual and thus very subjective and, depending on the wave quality, may give rise to large errors in the calculated velocities, especially considering the small distances involved (between source and receivers). However, results presented by Gillespie (1990) from DH SCPT data suggest that this technique is accurate and provides repeatable velocity measurements if the shear wave traces are of high quality with little noise present. The high quality of the shear wave traces results from the good coupling between the soil and the penetrometer.

Crossover method

Tanimoto & Kurzeme (1973) first suggested the idea of superimposing oppositely polarized shear wave traces for determining XH shear wave arrival times. Robertson, Campanella, Gillespie & Rice (1986) describe the application of the cross-over time to DH SCPT data and the use of the pseudo-interval method. The method can be applied to determine the time of shear wave arrival if only one receiver is used for the XH test, or can be used with the pseudo-interval method for the DH test. When two receivers are used in the DH or XH test, a true interval travel time is obtained. A typical digitally filtered polarized signal set at two adjacent depths for a DH SCPT is shown in Fig. 5.

Cross-correlation method

As opposed to the crossover method, which uses a single matched point, the cross-correlation method uses the complete time history of signals at adjacent depths to determine the interval travel time. The cross-correlation of signals at adjacent depths is accomplished by shifting the lower signal relative to the upper signal. The shift is performed in time steps equal to the time interval between the digitized points. At each time-step shift, the sum of the product of the two signal amplitudes is calculated. A plot of the sum, or

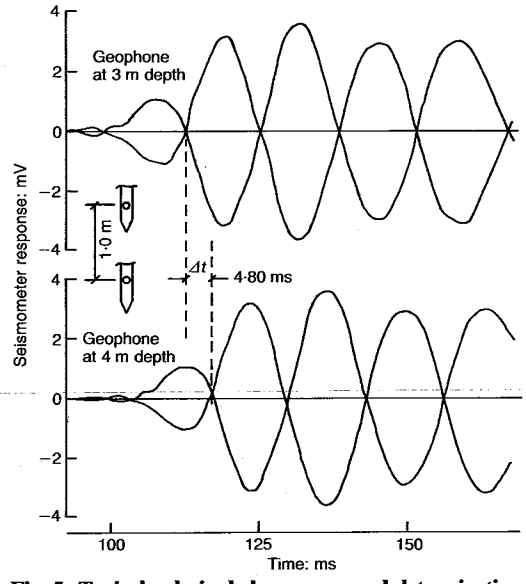

Fig. 5. Typical polarized shear waves and determination of interval travel time for DH SCPT (Robertson *et al.*, 1986)

cross-correlation, against time shift provides the time shift for the maximum cross-correlation. This time shift is used to calculate the interval velocity. The time shift of two adjacent signals to determine the interval time in the time domain and the resulting cross-correlation function are shown in Figs 6 and 7 respectively.

The cross-correlation is performed in the time domain. More efficiently, a fast Fourier transform (FFT) is used to convert the signal to the frequency domain. The cross-correlation of the signals is obtained using the inverse FFT of the product of the FFT of the upper signal and the complex conjugate of the lower. The signals are usually filtered using a zero phase shift digital filter before the cross-correlation procedure is performed. The frequency content for the shear wave signals generated is typically in the range 20–250 Hz. Filtering is performed using a 300 Hz low pass digital cosine filter.

Campanella, Baziw & Sully (1989) and Campanella & Stewart (1991) describe the method and the benefits of the cross-correlation technique applied to seismic cone testing, and compare the results of interpretation signals obtained from the crossover and cross-correlation methods. The interpreted shear wave velocities are essentially identical, the advantage of the cross-correlation technique being the elimination of judgemental error. All the shear wave velocities presented have been determined by application of both the crossover and the cross-correlation methods to digitally filtered signals.

The benefit of using two receivers in the XH test, and the similarity to the DH test, can be explained by reference to Fig. 8. In Fig. 8(a) the shear wave traces generated by the source S are recorded at successive depth intervals, as designated by receiver positions R1 and R2. If only R1 were available, the shear wave velocity would have to be interpreted from the first shear wave arrival and the velocity calculated using the direct wave travel path d_1. However, because a second reading is obtained when the cone receiver is pushed over the depth interval to R2, the wave traces at R1 and R2 can be interpreted using either the visual crossover method or the more

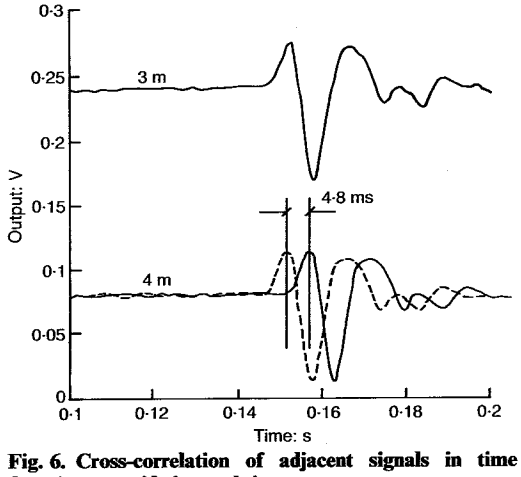

Fig. 6. Cross-correlation of adjacent signals in time domain to provide interval time

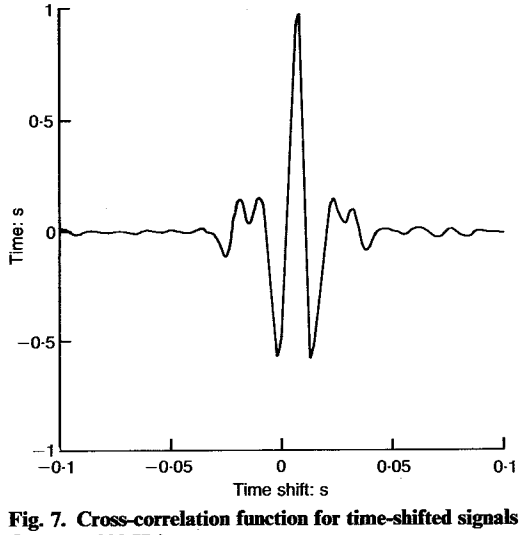

Fig. 7. Cross-correlation function for time-shifted signals (low pass 300 Hz)

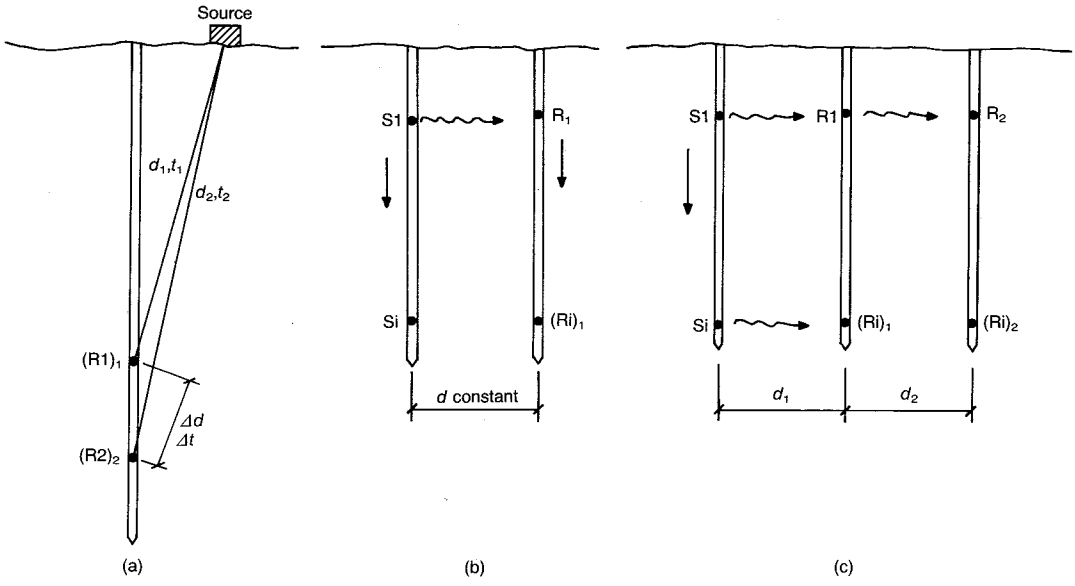

Fig. 8. Comparison of possible interpretation methods for DH and XH velocity measurements according to number of receivers used: (a) DH SCPT, cross-correlation possible from records at $(R1)_1$ and $(R2)_2$; (b) XH SCPT (one receiver), cross-correlation not possible; (c) XH SCPT (two receivers), cross-correlation possible for records at R1 and R2

complete cross-correlation method detailed below.

In the XH test, if only one receiver is used (Fig. 8(b)) only the first shear wave arrival can be used to estimate the velocity of propagation. However, if two receivers are used in the crosshole test, as in Fig. 8(c), then a complete interpretation of the data can be made. Hence, in terms of the possibilities for data interpretation, the XH test with two receivers can be regarded as a DH test with one receiver. The XH test with one receiver is the least desirable test set-up as the methods of data interpretation are limited, subjective and hence open to error.

THEORETICAL CONSIDERATIONS

Previous research has shown that, at small strains, V_s depends on both effective confining stress σ' and soil state or fabric

$$V_s = C_s(\sigma')^n \tag{3}$$

where C_s is a shear wave velocity constant dependent on soil state and n is the stress-dependent exponent. Little or no effect of over consolidation ratio has been found from laboratory data (Hardin & Drnevich, 1972; Lee, 1985). Recent results, however, suggest that V_s is also affected by the level of shear stress in the soil (Nishio & Tamaoki, 1990; Yan & Byrne, 1990). Roesler (1979) suggested that V_s depends primarily on the stresses in the direction of wave propagation and in the direction of particle motion, the third principal stress having a negligible effect on V_s, and proposed the individual stress index for describing the dependence of V_s on the level of effective stress, with the resulting relationship

$$V_s = C_s(\sigma_a')^{n_a}(\sigma_b')^{n_b}(\sigma_c')^{n_c} \tag{4}$$

where σ_a', σ_b', σ_c' are the principal effective stresses and n_a, n_b, n_c are exponents for each of the stress directions. The stress σ_a' acts in the direction of wave propagation, σ_b' acts in the direction of particle motion and σ_c' acts in the direction perpendicular to the wave propagation and motion.

Knox, Stokoe & Kopperman (1982) suggested the use of the average stress σ_m' index to demonstrate the dependence of V_s on stress level

$$\sigma_m' = (\sigma_a' + \sigma_b')/2 \tag{5}$$

and hence

$$V_s = C_s(\sigma_m')^{n_t} \tag{6}$$

The mean normal stress σ_0' can also be used to index the V_s dependence

$$\sigma_0' = (\sigma_a' + \sigma_b' + \sigma_c')/3 \tag{7}$$

whereby

$$V_s = C_s(\sigma_0')^{n_m} \tag{8}$$

The values of the exponents n_t and n_m depend on the stress terms used in the defined relationships.

Examination of equations (4), (6) and (8), however, shows that they are dimensionally incorrect. The relationships have been empirically derived based on laboratory test data, and most published results are presented in this way with little attention given to this fact. The constant C_s has units of velocity and so the stress term must be non-dimensional. This can be achieved by normalizing the stress term by atmospheric pressure p_a, as is the usual procedure. It would be simpler still to evaluate the stresses in units of bars, and hence $p_a = 1$. The value of C_s would then depend on the units used for V_s. However, as shown below, the stress terms are eliminated from the relationships when the XH and DH velocity ratios are calculated (see Appendix 1) and the dimensionality inconsistency is removed. The three effective stresses σ_a', σ_b' and σ_c' are considered to be principal stresses in order to evaluate the field data.

This study focuses on the use of in situ shear wave velocity measurements to evaluate anisotropy, using the relationships already presented. It is assumed that the generated shear waves are such that the planes of motion coincide with the principal stress directions and that the soil can be modelled as a cross-anisotropic medium, i.e. the vertical axis is an axis of symmetry. The above stress-dependent shear wave velocity relationships are consistent for cross-anisotropic elasticity where wave propagation is along principal stress directions. It is also assumed that a single shear wave velocity constant C can be used for the three-dimensional model (this is modified later to consider different values for the isotropic and anisotropic stress planes).

For the stress histories of the soils involved in this study and the vertical and horizontal orientation of the generated shear waves, this assumption is considered realistic. This model is used to interpret the field data in order to evaluate the controlling effects of induced and/or inherent anisotropy on shear wave velocity measurements.

In geophysical studies, various authors have suggested that in rock, the variation in velocity of the oriented shear waves is indicative of the anisotropy of the medium and sensitive to the material properties along the ray path (Crampin, 1977, 1981; Lynn, 1991). Similar findings have been published in the field of geotechnical engineering, but with emphasis on results from laboratory tests on reconstituted granular samples.

The simplest anisotropic model used for evaluating the measured shear wave velocities is that of cross-anisotropy. Based on a series of tests in a large cubical sand specimen, Lee (1985) suggests that equation (4) correctly models the characteristic cross-anisotropic behaviour of natural sands. A similar conclusion is reached by Yan & Byrne (1990) from V_s measurements in a hydraulic gradient similitude model.

Relations for DH and XH shear wave velocities

The stress–velocity relationships of equations (4), (6) and (8) can be rewritten in terms of K_0 for the evaluation of in situ field data, where K_0 is defined as

$$K_0 = \sigma_h'/\sigma_v' = \sigma_3'/\sigma_1' \tag{9}$$

Furthermore, it is assumed that the stresses in the horizontal plane are isotropic ($\sigma_2' = \sigma_3' = \sigma_h'$). Hence, the generated shear waves can be classified according to the planes in which propagation and particle motion occur.

Defined in this way, a shear wave propagating horizontally with particle motion in the horizontal plane can be considered as an isotropic shear wave as σ_h' is the only stress acting in the directions of propagation and particle motion, and is designated $(V_s)_I$. Conversely, any wave generated with the direction of propagation and particle motion in planes where the stresses are not isotropic can be designated the anisotropic shear wave, or $(V_s)_A$. The $(V_s)_A$ velocity, then, defines both the DH VH shear wave and the XH HV wave, whereas the $(V_s)_I$ velocity explicitly defines the XH HH shear wave. To differentiate the two $(V_s)_A$ velocities when evaluating the field data, the superscripts DH and XH are used to denote the DH and XH situations respectively. Under true cross-anisotropy, if the DH and XH shear wave velocities in the σ_h' and σ_v' directions are equally sensitive to the stress and the C_A values are identical ($C_A^{DH} = C_A^{XH}$), then $(V_s)_A^{DH}$ should be the same as $(V_s)_A^{XH}$. However, if the directional shear wave velocities are not equally sensitive to σ_h' and σ_v', then the DH and XH V_s values will differ.

The various relationships between the isotropic $(V_s)_I$ and anisotropic $(V_s)_A$ shear wave velocities for each of the stress indices given are presented in Appendix 1. The $\sigma'_{a,b,c}$ values have been written in terms of the vertical and horizontal effective stresses (σ_v' and σ_h'), as is usual for in situ data interpretation. The directions of wave propagation and particle motion associated with seismic shear waves from DH and XH tests are shown in Fig. 9.

Using equations (4), (6) and (8) the ratio between the anisotropic and isotropic shear wave velocities can be related to the lateral stress coefficient K_0. For the three possible stress indices, the following ratios in terms of K_0 are obtained (see Appendix 1)

$$\frac{(V_s)_A}{(V_s)_I} = \frac{C_A}{C_I}\,(\text{mean normal stress}) \tag{10}$$

$$\frac{(V_s)_A}{(V_s)_I} = \left(\frac{C_A}{C_I}\right)\left(\frac{1+K_0}{2K_0}\right)^{n_t} \text{ (average stress)} \quad (11)$$

$$\frac{(V_s)_A}{(V_s)_I} = \left(\frac{C_A}{C_I}\right)(K_0)^{-n_a} \text{ (individual stress)} \quad (12)$$

where C_A and C_I are the anisotropic and isotropic shear wave velocity constants. The ratio C_A/C_I can be considered to be indicative of the anisotropy of the material as it relates the isotropic and anisotropic shear wave velocity constants, independently of the stress conditions.

From equations (10)–(12) it appears feasible to evaluate the results of in situ DH and XH V_s measurements in terms of both stress-induced and structural (inherent) anisotropy. The problem then is one of determining the various constants in these equations.

As an initial estimate, the C_A/C_I ratio can be taken as unity. (Published data from Lee (1985) and Yan & Byrne (1990) give a range of values between 1·0 and 1·1.) A review of the reported values of the exponents in equations (11) and (12) is given by Stokoe *et al.* (1985) and Sully (1991).

DH AND XH SCPT RESULTS

DH and XH SCPTS were performed at three research sites: Lr 232 St and 200 St are clay sites where an overconsolidated (OC) crust becomes normally consolidated (NC) with depth, and Laing Bridge South (LBS) presents a granular profile to 14 m below ground level. At Lr 232 St the change to an NC clay profile is fairly smooth, whereas it is very abrupt at 200 St. (It was thought that the stress history variation at 200 St. would prove ideal for mapping using DH and XH shear wave velocities.) Also, if equations (10)–(12) were valid, the expectation was that the non-destructive measurements would be a useful technique for evaluating anisotropic stress conditions in sand. However, data are not presented for the LBS sand site as the results are inconsistent. In the initial tests, uncharacteristically low XH shear wave velocities were measured with a large scatter in the data. This is thought to be a consequence of the interbedded soft silts at this site. In a second series of tests, similar DH and XH velocities were obtained, even though the variation in V_s at any depth was of the order of 10–20%; this magnitude of variation makes it impossible to evaluate the possible effects of anisotropy on V_s in sand. At the clay sites, the dispersion in the data is very small and it appears that relevant conclusions can be drawn as to the possible effects of anisotropy on V_s.

Detailed information on the geotechnical properties of the soils at each of the sites mentioned is given by Sully (1991). Representative cone penetration resistance profiles for both of the clay sites to a depth of 10 m are shown in Fig. 10.

Shear wave velocity measurements

Lr 232 St. The measured in situ DH and XH shear wave velocities at Lr 232 St are shown in Fig. 11. Each data point corresponds to the average of four velocity determinations. The two DH profiles were performed at the locations of

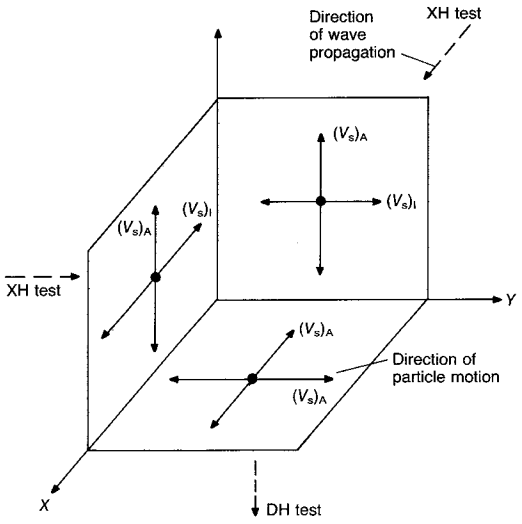

Fig. 9. Directions of wave propagation and particle motion for shear waves in DH and XH tests

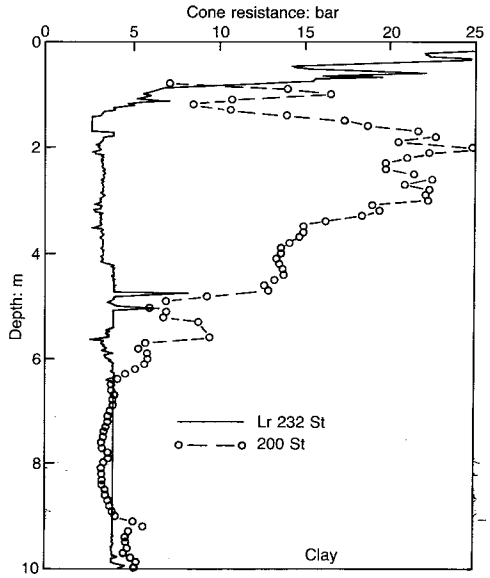

Fig. 10. CPT tip resistance profiles for sites tested

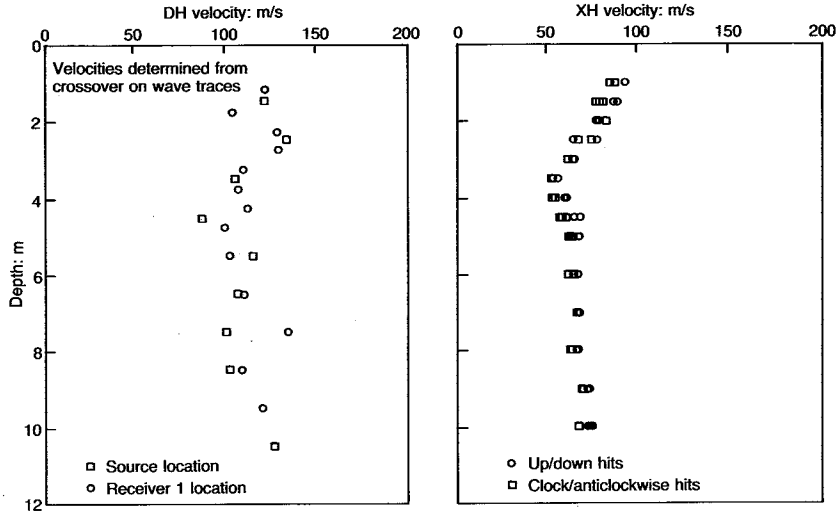

Fig. 11. DH and XH V_s profiles at Lr 232 St

the source cone and first receiver cone (R1) used for the XH set-up. A second receiver cone (R2) was used but problems were encountered with data capture, and so arrival times at R2 are not available for interpretation. Consequently, the XH V_s values are based on the first shear wave arrival (at receiver R1). Campanella *et al.* (1989) have shown that for the relatively homogeneous conditions at this site, good results can be obtained from this visual technique. DH velocities were calculated from crossover and cross-correlation travel times. Some scatter exists in the $(V_s)_{DH}$ values, but is confined to the upper 3 m of the profile. Below this depth, the DH shear wave velocities obtained at both locations agree well. All the DH shear waves are of the VH type described.

The $(V_s)^{XH}$ values in Fig. 11 have been obtained from two types of signal as already described. A hit in the up or down direction produces an HV

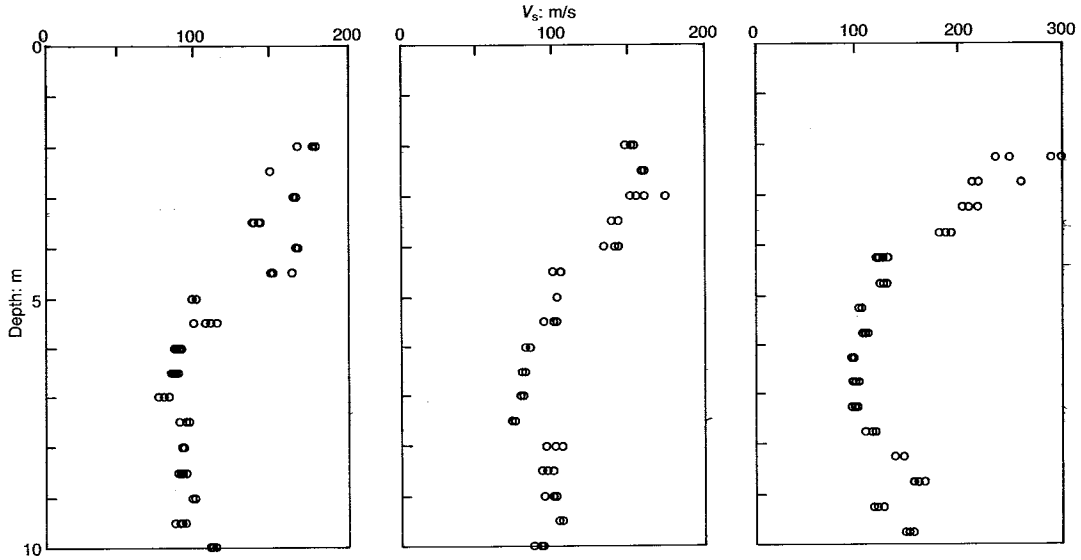

Fig. 12. DH and XH V_s profiles for 200 St: (a) XH V_s from crossover method, vertical up/down hits; (b) XH V_s from crossover method, left/right torque hits; (c) DH V_s from cross-correlation method

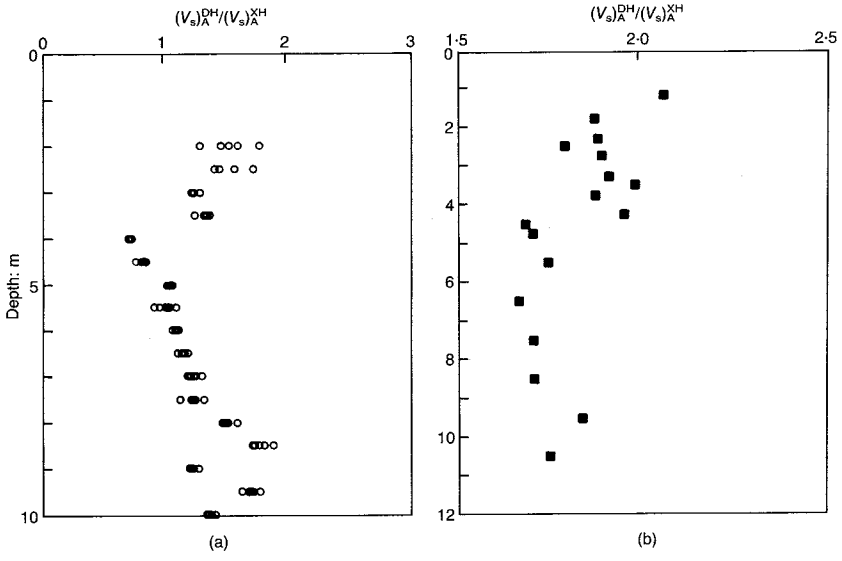

Fig. 13. Ratio of DH to XH $(V_s)_A$ from field measurements

shear wave, whereas the clockwise and anticlockwise (torque) hits produce HH shear waves. Fig. 11 shows that the two XH velocities are very similar, with a tendency for the VH velocity to be marginally larger than the HH velocity.

Both the DH and the XH velocity profiles indicate a degree of stress dependence. The high V_s at the surface reduces with depth to about 4 m before increasing linearly. This type of variation is typical for measurements of undrained shear strength—an accepted indicator of stress history (Schmertmann, 1975; Mayne & Mitchell, 1988)—in this type of deposit where OC surficial soils become NC with depth.

200 St. The DH and XH shear wave velocities determined at this site are shown in Fig. 12. The soil at 200 St is heavily to moderately overconsolidated (OCR = 5–20) to a depth of about 5 m. Below 5 m the clay silt is slightly overconsolidated (OCR = 2). The V_s profiles in Fig. 12 seem to reflect individually the stress history associated with the above description. The $(V_s)^{DH}$ is higher than both $(V_s)^{XH}$ values; the two XH velocities are again essentially identical. Two receiver cones were used at this site, so DH and XH velocity determination was done by both crossover and cross-correlation techniques.

Comparison of velocity ratios

In a cross-anisotropic material, it follows that if the stress dependence of V_s is the same in the two controlling directions (travel and particle motion), then the VH and HV shear wave velocities should be the same provided the two shear wave velocity constants are also identical ($C_A^{DH} = C_A^{XH}$), i.e.

$$(V_s)_A^{DH} = (V_s)_A^{XH} \tag{13}$$

This does not appear to be the case for any of the sites. However, this ratio appears to provide the best indicator of the known stress history profile for the sites (Fig. 13). For the Lr 232 St and 200 St clay data, it is clearly evident that (Figs 11 and 12)

$$(V_s)_I^{XH} = (V_s)_A^{XH} \tag{14}$$

and hence the stress relationships of equations (10)–(12) suggest that for this to be the case, either K_0 is constant with depth or the variation of V_s is not sensitive (relative to variations in C_I/C_A) to the in situ effective stress ratio.

DISCUSSION OF RESULTS

The theoretical relationships between velocity ratio and K_0 for the various stress indices are given in equations (10)–(12). The mean normal stress index suggests that the anisotropic to isotropic velocity ratio is solely a function of the ratio of the velocity constants in the two planes, and is independent of the effective stresses. The average stress (equation (11)) and individual stress (equation (12)) indices suggest a dependence on both the effective stress and velocity constants.

The theoretical variation of the velocity ratio $(V_s)_A/(V_s)_I$ with K_0 is shown in Fig. 14 for different values of the exponents in equations (11) and (12). Regarding these two plots (with $C_A/C_I = 1$), the following comments can be made.

(*a*) The average stress index in Fig. 14(a) appears to be a reasonable basis for using the velocity ratio concept to determine K_0 when $n_t > 0{\cdot}1$. Data from the literature suggest an average n_t value of 0·25 (Stokoe *et al.*, 1985).

(*b*) The individual stress index in Fig. 14(b) is unsuitable for determining K_0 irrespective of the n_a value. Small changes in the velocity ratio give large variations in predicted K_0, i.e. a $\pm 10\%$ change in the velocity ratio at $(V_s)_A/(V_s)_I = 1{\cdot}0$ gives a threefold variation in K_0.

An example of the insensitivity of the V_s ratio to variations in K_0 is given by the data at 200 St. The surface K_0 attains values of more than 2·0 in the OC soils, reducing to 0·6 in the underlying NC soils (Sully, 1991). Using equation (11) and (12), the variation in $(V_s)_A/(V_s)_I$ with depth for 200 St can be calculated. The results are shown in Fig. 15. Even at a site where the K_0 profile shows considerable variation, the V_s ratio is not suitable to index these changes.

While the shear wave velocity ratio $(V_s)_A/(V_s)_I$ does not appear to be sensitive to stress variations, it is interesting that the specific DH and XH shear wave velocities indicate stress-dependent effects and may provide an alternative route to obtaining information on K_0 changes. The drawback of this approach is that the shear wave velocity constant C (C_A or C_I) is required in order to back-calculate σ_h'.

As an example of this, the error in C was evaluated for the LBS data, where the in situ K_0 can be taken as 0·55 for the complete profile (Sully & Campanella, 1989). For $n_a = n_b = 0{\cdot}125$ and $n_t = 0{\cdot}25$ in equations (11) and (12), the same average back-calculated value of C was obtained from the average stress and individual stress methods

$C_{avg} = 59{\cdot}23$

standard deviation of $C_{avg} = 6{\cdot}62$

However, if $C = 59{\cdot}23$ is applied to the field data, then the statistics for K_0 for average stress are

$(K_0)_{avg} = 0{\cdot}594$

standard deviation of $(K_0)_{avg} = 0{\cdot}678$

and for individual stress are

$(K_0)_{avg} = 0{\cdot}751$

standard deviation of $(K_0)_{avg} = 0{\cdot}605$

Obviously, a single value of C may be used to obtain a global value of K_0 only for a complete profile and not for indexing changes with depth, especially in a deposit like this, where there is large scatter in the data. Furthermore, the cor-

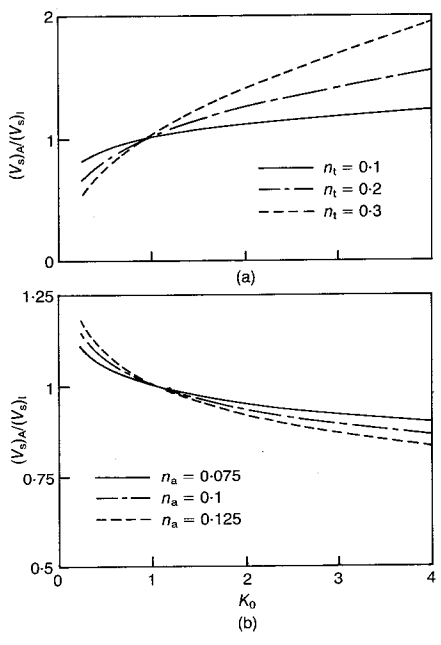

Fig. 14. Theoretical dependence of $(V_s)_A/(V_s)_I$ on K_0; $C_A/C_I = 1$: (a) average stress index; (b) individual stress index

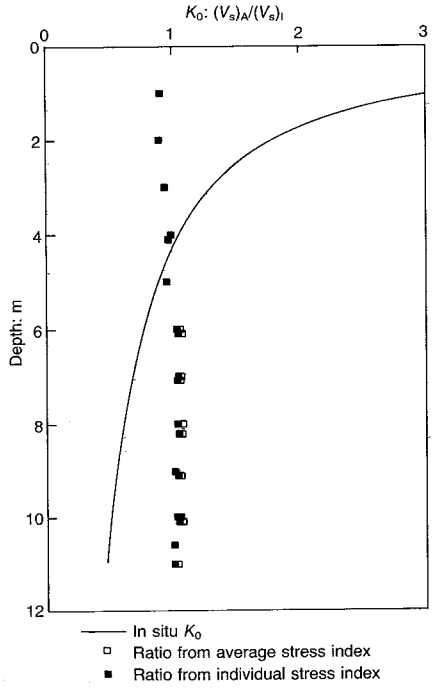

Fig. 15. Profile of K_0 and $(V_s)_A/(V_s)_I$ at 200 St: $C_A/C_I = 1$

rectness of this global value in terms of the 'true' K_0 is difficult to ascertain.

Another possibility for evaluating in situ stress conditions lies in combining laboratory and field data. Dobry & Vucetic (1987) evaluate laboratory and field measurements of V_s in various types of soil and show that the variation is of the order of $\pm 10\%$. Depending on the stress index used, the effect on σ_h' will be about 20%. This magnitude of error is considered acceptable by the Authors for most field situations, especially in terms of the effect of this variation on the engineering behaviour of soils.

In resonant column tests performed on isotropically consolidated samples from Lr 232 St (Zavoral, 1990) the relationship

$$G_{max} = 292{\cdot}1(p_a')^{0{\cdot}1}(\sigma_3')^{0{\cdot}9} \quad (15)$$

was obtained from which $V_s(=(G_{max}/\rho)^{0{\cdot}5})$ can be calculated. In equation (15), p_a' is the atmospheric pressure ($p_a' = 1$ bar $= 100$ kPa).

For stress ratios of less than 2·5, the deviatoric component of stress has a negligible effect on V_s (Hardin & Black, 1968), and the shear wave velocities from isotropic stress conditions can be equated to the same level of mean normal stress, i.e. σ_3' can be substituted by σ_0' or σ_{av}'.

The variation of the normalized shear modulus and damping with the level of shear strain is shown in Fig. 16 (G at higher shear strains has been determined from direct simple shear tests). Two profiles of K_0, determined using two different stress indices with both laboratory and field data as discussed above, are shown in Fig. 17 for Lr 232 St. Below 5 m, the K_0 values agree well with reference values obtained from total stress cells (TSC data), laboratory lateral stress (LS) oedometers and the Mayne & Kulhawy (1982) empirical correlation based on plasticity index (PI = 20). The stress indices σ_m' and σ_0' used for back-calculating K_0 are as defined in equations (5) and (7). Above 5 m, calculated values become progressively higher than the reference values as the ground surface is approached. This may arise due to the effect of OCR and shear stress, which is not considered in equation (13), or errors in V_s in the near-surface soils. Otherwise the results are promising.

Due to a lack of resonant column data, it was not possible to apply this approach at the other sites mentioned.

CONCLUSIONS

Based on the results presented for the two sites tested, it can be concluded that the shear wave velocity ratio $(V_s)_A/(V_s)_I$ is influenced only slightly by changes in the in situ effective stress conditions, but is much more sensitive to variations in the velocity constant ratio C_A/C_I. In this case, the DH/XH shear wave velocity ratio may provide a good indicator of structural (inherent) anisotropy rather than stress anisotropy. Hence, from the relationships in equations (10)–(12), it appears reasonable to use the mean normal stress as the stress index for evaluating field data, as this index

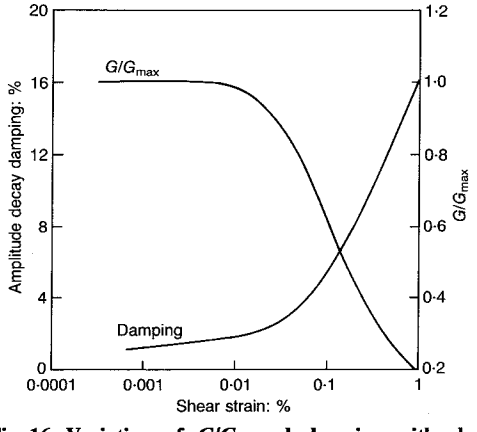

Fig. 16. Variation of G/G_0 and damping with shear strain for Lr 232 St (after Zavoral, 1990)

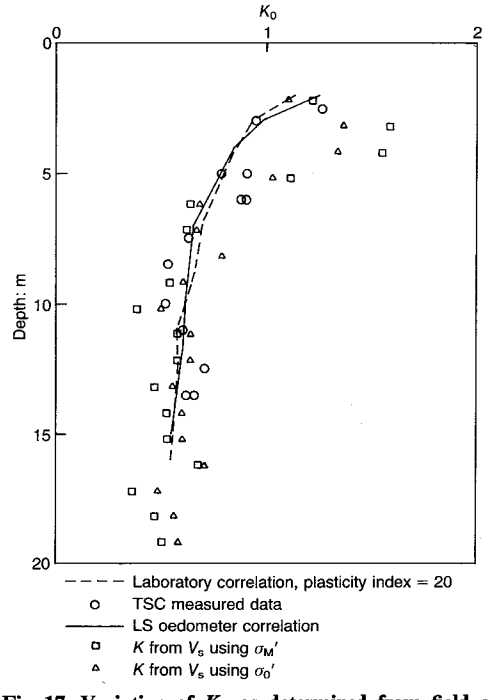

Fig. 17. Variation of K_0 as determined from field and laboratory V_s measurements (Lr 232 St)

is not influenced by variations in the effective stress conditions.

In contrast, the specific shear wave velocity measurements (DH or XH) indicate variations which are in accordance with the stress history at both of the sites tested. However, to interpret these measurements the velocity constants (C_I or C_A) must be determined.

As a possible approach to this problem, it appears that the combination of field and laboratory V_s data may provide realistic K_0 values. However, in sands and OC clays, the method may require a more complete definition of equation (13) and recovery of high-quality undisturbed samples if reasonable results are to be obtained.

An alternative reason for the poor correlation between velocity ratio and K_0 obtained from these field data may be that the use of a cross-anisotropic model is incorrect for the sites tested. If this is so, to interpret in situ stress conditions it would be necessary to provide additional measurements of shear wave velocity in directions oblique to the principal stress axes. This complication may render the technique unpractical for field applications.

The application of shear wave velocity measurements to the determination of in situ stress conditions requires further validation from both laboratory and field measurements. This research will undoubtedly be fuelled by the possibility of using testing techniques involving very small strain levels for the evaluation of a soil parameter that corresponds, by definition, to a zero strain condition. In contrast, current practice induces varying degrees of disturbance to the soil, as in situ determination involves installation in the ground of some type of probe for stress measurement.

NOTATION

C_A	shear wave velocity constant in anisotropic plane
C_I	shear wave velocity constant in isotropic plane
C_s	shear wave velocity constant
G	shear modulus
G_0, G_{max}	maximum (small strain) shear modulus
K	coefficient of lateral stress
K_0	coefficient of lateral stress at rest
p_a	atmospheric pressure
n_a, n_b, n_c	exponents for V_s–σ' relationship in terms of individual stresses
n_m	exponents for V_s–σ' relationship in terms of average stress
n_t	exponents for V_s–σ' relationship in terms of mean normal stress
V_s	shear wave velocity
$(V_s)_A$	shear wave velocity in anisotropic plane
$(V_s)_I$	shear wave velocity in isotropic plane
α	factor related to soil fabric
ρ	bulk density
σ_1', σ_2', σ_3'	effective principal stresses
σ_h', σ_v'	horizontal, vertical effective stress

ACKNOWLEDGEMENTS

The Authors are grateful to S. Jackson and A. Brookes for assistance with the equipment used, and to Dr W. P. Stewart for discussions on the data processing. Financial assistance from the Natural Sciences and Engineering Research Council of Canada, the University of British Columbia Graduate Fellowship Program and INTEVEP, S.A. is also acknowledged.

APPENDIX 1. V_s STRESS RELATIONSHIPS

By combining the general equation

$$V_s = C_s(\sigma_i') \tag{16}$$

with the various stress indices and rearranging, the relationships between V_s and K_0 can be obtained. The ratio of the DH to XH shear wave velocities is then derived as follows.

Mean normal stress

For the DH test with VH wave or the XH test with HV wave, and assuming $(C_A)^{DH} = (C_A)^{XH}$

$$V_s = (C_A)^{DH}(\sigma_0')^{n_m} \tag{17}$$

For the XH test with HH wave

$$V_s = (C_I)^{XH}(\sigma_0')^{n_m} \tag{18}$$

The exponents in the DH and XH are assumed to be the same. The shear wave velocity is also considered independently of the orientation of the two stresses in the planes of propagation and particle motion. Hence the ratio of anisotropic (DH VH or XH HV) to isotropic (XH HH) shear wave velocities can be written as in equation (10).

Average stress

$$(V_s)_A = C_A\left(\frac{\sigma_v' + \sigma_h'}{2}\right)^{n_t} = C_A(\sigma_v')^{n_t}\left(\frac{1 + K_0}{2}\right)^{n_t} \tag{19}$$

$$(V_s)_I = C_I\left(\frac{\sigma_h' + \sigma_h'}{2}\right)^{n_t} = C_I(\sigma_v')^{n_t}(K_0)^{n_t} \tag{20}$$

Equation (20) applies where particle motion and propagation are in the horizontal plane.

Individual stress

$$(V_s)_A = C_A(\sigma_v')^{n_a}(\sigma_h')^{n_b}$$
$$= C_A(\sigma_v')^{n_a+n_b}(K_0)^{n_b} \quad (21)$$
$$(V_s)_I = C_I(\sigma_h')^{n_a}(\sigma_h')^{n_b}$$
$$= C_I(K_0\sigma_v')^{n_a+n_b} \quad (22)$$

REFERENCES

Baldi, G., Bruzzi, D., Superbo, S., Battaglio, M. & Jamiolkowski, M. (1988). Seismic cone in Po River sand. *Proceedings of international symposium on penetration testing, ISOPT-1, Orlando*, vol. 2, pp. 643–650. Rotterdam: Balkema.

Campanella, R. G., Baziw, E. J. & Sully, J. P. (1989). Interpretation of seismic cone data using digital filtering techniques. *Proc. 12th Int. Conf. Soil Mech. Rio de Janeiro* **1,** 195–198. Rotterdam: Balkema.

Campanella, R. G. & Robertson, P. K. (1981). Applied cone research. *Proceedings of symposium on cone penetration and experience*, pp. 343–362. New York: American Society of Civil Engineers.

Campanella, R. G. & Robertson, P. K. (1984). A seismic cone penetrometer to measure engineering properties of soil. *Proc. 54th Ann. Mtg Soc. Exploration Geophys, Atlanta.*

Campanella, R. G., Robertson, P. K. & Gillespie, D. G. (1986). Seismic cone penetration test. *Proceedings of in situ '86, Blacksburg*, pp. 116–130. New York: American Society of Civil Engineers.

Campanella, R. G. & Stewart, W. P. (1991). Seismic cone analysis using digital signal processing. *Proc. 2nd Int. Conf. Recent Adv. Geotech. Earthquake Engng Soil Dyn., St Louis* **1,** 77–82.

Crampin, S. (1977). A review of the effects of anisotropic layering on the propagation of seismic waves. *Geophys. J. Roy. Astr. Soc.* **53,** No. 1, 9–27.

Crampin, S. (1981). A review of wave motion in anistropic and cracked media. *Wave Motion* **3,** 343–391.

Dobry, R. & Vucetic, M. (1987). Dynamic properties and seismic response of soft clay deposits. S-O-A Report. *Proceedings of international symposium on geotechnical engineering of soft soils, Mexico*, vol. 2, pp. 49–85.

Gillespie, D. G. (1990). *Evaluating shear wave velocity and pore pressure data from the seismic cone penetration test.* PhD thesis, University of British Columbia.

Hardin, B. O. (1978). The nature of stress–strain behaviour of soils. *Proceedings of conference on earthquake engineering and soil dynamics, Pasadena*, vol. 1, pp. 3–29. New York: American Society of Civil Engineers.

Hardin, B. O. & Black, A. M. (1968). Vibration modulus of normally consolidated clay. *Proc. J. Soil Mech. Fdn Engng Div. Am. Soc. Civ. Engrs* **94,** SM2, 353–369.

Hardin, B. O. & Drnevich, V. P. (1972). Shear modulus and damping in soils: design equations and curves. *Proc. J. Soil Mech. Fdn Engng Div. Am. Soc. Civ. Engrs* **98,** SM7, 667– 691.

Knox, D. P., Stokoe, K. H. & Kopperman, S. E. (1982). *Effect of state of stress on velocity of low amplitude shear waves propagating along principal stress directions in dry sand.* Report GR88-23, University of Texas at Austin.

Lee, S. H. H. (1985). *Investigation of low amplitude shear wave velocity in anisotropic material.* PhD thesis, University of Texas at Austin.

Lynn, H. B. (1991). Field measurements of azimuthal anisotropy: first 60 meters, San Francisco Bay area, CA, and estimation of the horizontal stresses ratio from V_{s1}/V_{s2}. *Geophysics* **56,** No. 6, 822–832.

Mayne, P. W. & Kulhawy, F. (1982). K_0–OCR relationships in soil. *J. Geotech. Engng Div. Am. Soc. Civ. Engrs* **108,** GT6, 851–872.

Mayne, P. W. & Mitchell, J. K. (1988). Profiling of overconsolidation ratio in clays by field vane. *Can. Geotech. J.* **25,** No. 1, 150–157.

Nazarian, S. & Stokoe, K. H. (1984). In situ shear wave velocities from spectral analysis of surface waves. *Proc. 8th Wld Conf. Earthquake Engng, San Francisco* **3,** 31–38.

Nishio, S. & Tamaoki, K. (1990). Stress dependency of shear wave velocities in diluvial gravel samples during triaxial compression tests. *Soils Fdns* **30,** No. 4, 42–52.

Robertson, P. K., Campanella, R. G., Gillespie, D. & Rice, A. (1986). Seismic CPT to measure in situ shear wave velocity. *J. Geotech. Engng Div. Am. Soc. Civ. Engrs* **112,** No. 8, 791–804.

Roesler, S. K. (1979). Anisotropic shear modulus due to stress anisotropy. *J. Geotech. Engng Div. Am. Soc. Civ. Engrs* **105,** GT5, 871–880.

Schmertmann, J. H. (1975). Measurement of in situ shear strength. *Proceedings of international symposium on measurement of soil properties, Raleigh*, vol. 2, pp. 57–138. New York: American Society of Civil Engineers.

Stokoe, K. H., Lee, S. H. H. & Knox, D. P. (1985). Shear moduli measurement under true triaxial stresses. *Proceedings of symposium on advances in testing of soils under cyclic conditions*, pp. 166–185. New York: American Society of Civil Engineers.

Stokoe, K. H. & Nazarian, S. (1985). Use of Rayleigh waves in liquefaction studies. In *Measurements and use of shear wave velocity for evaluating dynamic soil properties.* New York: American Society of Civil Engineers.

Stokoe, K. H. & Woods, R. D. (1972). In situ shear wave velocity by cross-hole method. *J. soil Mech. Fdn Engng Div. Am. Soc. Civ. Engrs* **99,** No. 5, 443–459.

Sully, J. P. (1991). *Measurement of in situ lateral stress during full-displacement penetration tests.* PhD thesis, University of British Columbia.

Sully, J. P. & Campanella, R. G. (1989). Correlation of maximum shear modulus with DMT test results in sand. *Proc. 12th Int. Conf. Soil Mech. Fdn Engng, Rio de Janeiro* **2,** pp. 339–343.

Sully, J. P. & Campanella, R. G. (1992). In situ shear wave velocity determination using seismic cone penetrometer for evaluating soil anisotropy. *Proc. 10th Wld Conf. Earthquake Engng, Madrid* **3,** 1269–1274.

Tanimoto, K. & Kurzeme, M. (1973). Discussion on In situ shear wave velocity by cross-hole method, by K. H. Stokoe and R. D. Woods (1972). *J. Soil Mech. Fdn Engng Div. Am. Soc. Civ. Engrs* **99,** 351–353.

Woods, R. D. (1978). Measurement of dynamic soil properties. *Proceedings of conference on earthquake*

engineering and soil dynamics, Pasadena, vol. 1, pp. 91–178. New York: American Society of Civil Engineers.

Woods, R. D. (1986). In situ tests for foundation vibrations. *Proceedings of in situ '86, Blacksburg*, pp. 336–375. New York: American Society of Civil Engineers.

Woods, R. D. (1991). Field and laboratory determination of soil properties at low and high strains. *Proc. 2nd Int. Conf. Recent Adv. Geotech. Earthquake Engng Soil Dyn., St Louis* **2,** 1727–1741.

Yan, L. & Byrne, P. M. (1990). Simulation of downhole and crosshole seismic tests on sand using hydraulic gradient similitude method. *Can. Geotech. J.* **27,** No. 4, 441–460.

Yu, P. & Richart, F. E. (1984). Stress ratio effects on shear modulus for sand. *J. Geotech. Engng Div. Am. Soc. Civ. Engrs* **110, 3,** 331–345.

Zavoral, D. Z. (1990). *Dynamic properties of an undisturbed clay from resonant column tests.* MASc thesis, University of British Columbia.